NIH Public Access
Author Manuscript
J Polym Sci A Polym Chem. Author manuscript; available in PMC 2009 October 22.

Published in final edited form as:
J Polym Sci A Polym Chem. 2008 ; 46(22): 7578–7583. doi:10.1002/pola.23020.

Folate-mediated Cell Uptake of Shell-crosslinked Spheres and Cylinders

Ke Zhang, **Raffaella Rossin**, **Aviv Hagooly**, **Zhiyun Chen**, **Michael J. Welch***, and **Karen L. Wooley***
Department of Chemistry, Washington University, 1 Brookings Drive, St. Louis, Missouri 63130; Department of Radiology, Washington University School of Medicine, 510 South Kingshighway Boulevard, St. Louis, Missouri 63110

Abstract

This paper reports the synthesis of shell crosslinked nanoparticles (SCKs) of spherical and cylindrical shapes, and their functionalization with folate using a poly(ethylene glycol) (PEG) construct that has folate and an amine group as the opposing chain termini. By use of confocal microscopy, we demonstrate the selective delivery of folate conjugated SCKs to human KB cells, a cell line that overexpresses the folate receptor (FR). A higher extent of polymer uptake by the cells occurred with the cylindrical SCK morphology, relative to the spherical SCKs, when both samples had the same fluorescein-5-thiosemicarbazide and polymer concentrations. In both cases, by using excess free folic acid as a block or SCKs lacking the folate-PEG conjugate, cell uptake was significantly reduced. These results suggest that particle shape may play an important role in receptor-mediated cell uptake, and may be exploited in the targeted delivery of nanoscopic drugs.

Keywords

shape; size; folic acid; nanoparticle; shell-crosslink; rod-shaped; sphere

INTRODUCTION

Thus far, most drugs approved for clinical use function in an indiscriminate fashion they access pathologic and healthy tissues alike. As a result, the effect of the drug is systemic rather than specific. The ability of a therapeutic or diagnostic agent to preferentially localize at diseased tissues would, therefore, be of great value. Towards this end, polymeric nanoparticles have been designed and synthesized to augment the drug's local concentration.[1–5] As an interesting targeted nanoparticle example, Hubbell *et al.* have developed a drug delivery system with dual targeting moieties, which led to up to a 72-fold increase in targeting to the extracellular compartment of articular cartilage in mice.[6] Although significant progress has been made in terms of identifying the targets and construction of targeting nanoparticles, the shape effect of the nanoparticle platform *per se* on cell binding and internalization through receptor-ligand interactions has not yet been investigated thoroughly.[7,8] Our interest here is to synthesize nanoparticles of different shapes and sizes, and use a well-known receptor-ligand pair to study whether the shape effects exist, and if they do, which shape is more favorable for this particular receptor-ligand pair.

In our study, folate was used as the model targeting ligand to be conjugated to the nanoparticles. Folate has received extensive study as a targeting device for proteins utilizing

Corresponding authors: welchm@mir.wustl.edu, klwooley@wustl.edu.

NIH-PA Author Manuscript
NIH-PA Author Manuscript
NIH-PA Author Manuscript

NIH-PA Author Manuscript

NIH-PA Author Manuscript

NIH-PA Author Manuscript

folate receptor (FR)-mediated endocytosis.9 By virtue of its high binding affinity towards the cell surface FR, which is overexpressed in a number of pathologic cells, selective delivery of non-specific drugs that are conjugated to folate can be achieved. Derivatization of folate has been successfully exploited in the targeted delivery of proteins,10,11 liposomes,12 DNA nanoparticles,13,14 synthetic organic15,16 and inorganic nanoparticles, 17,18 and polymers.19 As a targeting ligand, folate has many important advantages compared to monoclonal antibodies, such as low immunogenicity, high specificity and resistance to denaturation, *etc*. Moreover, FR targeting agents may continuously accumulate into the cells due to receptor recycling. Finally, folic acid has two carboxylic acid groups, one that is sterically blocked and the other that allows for simple and defined conjugation to a variety of organic molecules and nanoparticles through amidation chemistry. Herein, we report a method to create spherical and cylindrical polymer shell-crosslinked (SCK) nanoparticles20 of similar chemical compositions, and to functionalize these nanoparticles with folic acid through a PEG tether. We then further demonstrate that both nanoparticles received enhancement in uptake by human KB cells, surprisingly, with the cylindrical nanostructures being internalized to a greater extent than the spheres, and this enhancement could be competitively blocked partially by free folic acid.

EXPERIMENTAL

Polymer synthesis

The two amphiphilic block copolymers used in this study were prepared by atom transfer radical polymerization, using literature procedures.21

Spherical SCK formation

The spherical polymer micelle sample was prepared by dissolving 18.6 mg of the block copolymer, poly(acrylic acid)$_{128}$-*b*-polystyrene$_{40}$ (PAA$_{128}$-b-PS$_{40}$) in 20 mL dimethylformamide (DMF) followed by slow addition (4.0 mL/h) of an equal volume of nonsolvent (H_2O) for the hydrophobic polystyrene to induce micellization. The micelles were stirred for 4 h before being transferred to presoaked dialysis tubing (MWCO 6–8 kDa) and dialyzed against nanopure water (18.0 MΩ·cm) for 3 days to remove the organic solvent. The final volume was 66 mL of aqueous micelle solution for a final concentration of 0.28 mg/mL. Transmission electron microscopy (TEM): 10 ± 1 nm (diameter). Dynamic light scattering (DLS): 14 ± 2 nm (diameter). The aqueous micelle solution was then mixed with *O*-bis-(aminoethyl)ethylene glycol (0.20 equiv., relative to the molar number of available COOH groups) and allowed to stir at room temperature. After 30 min, an aqueous solution of 1-[3′-(dimethylamino)propyl]-3-ethylcarbodiimide hydrochloride (EDCI) (1 equiv., relative to the molar number of available COOH groups) was added. The reaction mixture was allowed to stir overnight before being transferred to presoaked dialysis tubing (MWCO 3 kDa) and dialyzed against nanopure water (18.0 MΩ·cm) for 3 days.

Cylindrical SCK formation

To a stirring solution of 8.4 mg triblock copolymer, poly(acrylic acid)$_{94}$-*b*-poly(methyl acrylate)$_{103}$-*b*-polystyrene$_{28}$ (PAA$_{94}$-*b*-PMA$_{103}$-*b*-PS$_{28}$) in 8.00 mL tetrahydrofuran (THF) was added a solution of THF (2.0 mL) containing O-bis-(aminoethyl)ethylene glycol (0.20 equiv., relative to COOH groups). The mixture was allowed to stir overnight at room temperature, and then H_2O (40 mL) was added at a rate of 7.00 mL/h to induce micellization. To this water-THF mixture, EDCI (6.3 mg) was added to crosslink the shell domain of the micelle and to lock the morphology.22 After stirring overnight, the reaction mixture was transferred to presoaked dialysis tubing (MWCO 6–8 kDa) and dialyzed against nanopure water (18.0 MΩ·cm) for 3 days to remove the organic solvent and other residues. The final volume was 62.6 mL of aqueous crosslinked long, cylindrical micelle solution for

NIH-PA Author Manuscript

NIH-PA Author Manuscript

NIH-PA Author Manuscript

a final concentration of 0.13 mg/mL. TEM: 900 nm (length) and 30 ± 2 nm (cross-sectional diameter).

Functionalization with fluorescent tag

The SCK solutions were diluted to the same polymer concentration (6.9 μM) and each was placed into a round-bottom flask and cooled to 0 °C using an ice bath. A solution of 1:1 (mole : mole) EDCI : *N*-hydroxysulfosuccinimide (sulfo-NHS) was added to each nanoparticle solution (0.5 : 1 molar ratio, relative to the available COOH groups) to activate the acrylic acid residues. After 30 minutes, the pH of the reaction mixtures was adjusted to 7.7 using pH = 8.0 sodium bicarbonate solution. Then, aliquots of fluorescein-5-thiosemicarbazide stock solution were added to each flask and the mixtures were allowed to react overnight. The solutions were then transferred to presoaked dialysis tubings (MWCO 6–8 kDa) and allowed to dialyze for 3 days against 150 mM NaCl solution, then for 3 days against nanopure water.

Conjugation of folate-PEG(1.5 kDa)-amine to nanostructures

The folate-PEG(1.5 kDa)-amine construct was synthesized by coupling of bis-PEG-amine (MW 1.5 kDa) with folic acid, according to a literature procedure.[23–25] Conjugation to the nanostructures was achieved by use of amidation chemistry. SCK solutions pre-functionalized with fluorescein-5-thiosemicarbazide were each placed into a 25 mL round-bottom flask. Sodium chloride was placed into each flask to give a concentration of 5.0 mg/mL, to minimize particle-particle aggregation. The flasks were then placed in an ice bath. A mixed solution of 1 : 1 (mole : mole), EDCI : sulfo-NHS was added to each nanoparticle solution (0.7 : 1 molar ratio, relative to the available COOH groups) to activate the acrylic acid residues. Aliquots of the folate-PEG-amine DMF solution (14.3 mg/mL, 10.0 equiv. to polymer) were added to the respective flasks 30 min after the addition of EDCI/NHS. The pH of each reaction mixture was adjusted to 7.4 using pH = 8.0 sodium bicarbonate solution. The mixtures were allowed to react overnight. The solutions were then transferred to presoaked dialysis tubings (MWCO 12 kDa) and allowed to dialyze against nanopure water for 5 days, then against pH =7.4 PBS buffer for 2 days. UV-Vis measurements confirmed coupling of the folate-PEG-amine to the SCKs (Figure 2).

Transmission Electron Microscopy

Samples for TEM measurements were diluted with a 1 % phosphotungstic acid (PTA) stain (v/v, 1:1). Carbon grids were exposed to oxygen plasma treatment to increase the surface hydrophilicity. Micrographs were collected at 10,000, 20,000, 50,000, and 100,000 × magnification and calibrated using a 41 nm polyacrylamide bead from NIST.

Dynamic Light Scattering

Hydrodynamic diameter (D_h) and size distribution for the spherical SCK were determined by DLS. The DLS instrumentation consisted of a Brookhaven Instruments Limited (Worcestershire, U.K.) system, including a model BI-200SM goniometer, a model BI-9000AT digital correlator, a model EMI-9865 photomultiplier, and a model 95-2 Ar ion laser (Lexel Corp.) operated at 514.5 nm. Measurements were made at 25 ± 1 °C. Scattered light was collected at a fixed angle of 90°. The digital correlator was operated with 522 ratio spaced channels, and initial delay of 5 μs, a final delay of 100 ms, and a duration of 10 minutes. A photomulitplier aperture of 400 μm was used, and the incident laser intensity was adjusted to obtain a photon counting of between 100 and 200 kcps. Only measurements in which the measured and calculated baselines of the intensity autocorrelation function agreed to within 0.1 % were used to calculate particle size. The calculations of the particle size distributions and distribution averages were performed with the ISDA software package

NIH-PA Author Manuscript

NIH-PA Author Manuscript

NIH-PA Author Manuscript

(Brookhaven Instruments Company), which employed single-exponential fitting, cumulants analysis, and CONTIN particle size distribution analysis routines. All determinations were repeated 5 times.

Cell Line and Fluorescence Confocal Microscopy

KB cells were obtained from American Type Culture Collection and cultured continuously as a monolayer at 37 °C in a humified atmosphere containing 5% CO_2 in folate-deficient modified Eagle's medium (FDMEM) (a folate-free modified Eagle's medium supplemented with 10% [v/v] heat-inactivated fetal bovine serum as only source of folate) containing 2 mmol/L L-glutamine. 24 h prior to the assay, KB cells in FDMEM were transferred to 33 mm culture dishes at 3×10^5 cells per dish, and were rinsed with PBS (1 mL) and incubated for 4 h at 37 °C with each of the four SCK solutions (spherical/cylindrical, with/without folate) diluted 10 times by culture medium. In free folate competition studies, 1 mmol/L folic acid was added to the incubation medium. After washing with PBS (3 × 1 mL) to remove free nanoparticles, cell-associated fluorescence was imaged by confocal microscopy (Leica TCS SP2 inverted microscope). An argon laser for FTSC excitation at 488 nm was used for imaging. All imaging settings including laser power were kept identical throughout the study for all samples.

RESULTS AND DISCUSSION

The overall design in this study involved the use of well-defined amphiphilic block copolymers to form micelles of a core-shell architecture. Due to the inherent differences in the block copolymers and the micellization conditions, different morphologies of the resulting micelles could be obtained. After shell crosslinking of the micelles using a diamine crosslinker, their respective morphologies were locked.22 Then, a folic acid derivative, folate-PEG-amine, was conjugated to the shell-crosslinked nanoparticles, and the conjugates were evaluated in cells (Scheme 1). The syntheses of the amphiphilic diblock copolymer PAA_{128}-*b*-PS_{40} and triblock copolymer PAA_{94}-*b*-PMA_{103}-*b*-PS_{28}, were achieved using atom transfer radical polymerization, following previously reported methods.21 The block copolymers were then dissolved in a good solvent for both/all blocks (THF or DMF), followed by slow addition of water to induce micellization. The two resulting micelle samples exhibited distinctive morphologies, spherical and rod-shaped, from the diblock and triblock copolymers, respectively. To impart stability to these micelles, such that under cell incubation fluid conditions the micelles do not disassemble into discrete polymer chains, crosslinking in the shell domain of the micelle using 2, 2′-(ethylenedioxy)bis(ethylamine) was performed with the aid of EDCI, consuming 20% of available carboxylic acids on the micelle.21 The shell was also fluorescently labeled with fluorescein to enable particle tracking. The polymer and fluorescein concentrations for each sample were controlled to be approximately the same (Figure 2), thus allowing direct comparison of cell uptake by examining the confocal fluorescent images. The shell-crosslinked nanoparticles were characterized by DLS and TEM (Figure 1). DLS gave a mean diameter of 14 ± 2 nm for the spherical SCK, while TEM gave 10 ± 1 nm. For the cylindrical SCK, TEM gave a mean length of 900 nm, and a mean cross-sectional diameter of 30 ± 2 nm.

Attachment of folic acid to the surface of the SCKs was achieved through the same carbodiimide coupling chemistry as was employed for the crosslinking reactions. A PEG(1.5 kDa) linker was used to tether folate to the nanoparticle, since direct attachment of folic acid to nanostructures has been reported to result in reduced binding of folic acid to FR, possibly due to steric effects that limit folate from reaching the binding pockets of FR.26 The synthesis of folate-PEG-amine followed previously reported methods.23–25 The conjugates showed UV absorptions at 363 nm, representative of folate. The extinction coefficient for

NIH-PA Author Manuscript

NIH-PA Author Manuscript

NIH-PA Author Manuscript

folate in pH 7.4 PBS buffer at that wavelength is 6197 $M^{-1}cm^{-1}$. The number of folates per polymer can therefore be calculated as follows:

Folates/polymer = (Abs. at 363 nm/6197 $M^{-1}cm^{-1}$)/[polymer (mg/mL)]/(MW of polymer (g/mol)) For PAA_{128}-*b*-PS_{40}, which forms the spherical particle, the folate/polymer number was determined to be 3.2; for PAA_{94}-*b*-PMA_{103}-*b*-PS_{28}, which forms the cylindrical particle, the folate/polymer number was determined to be 3.0. As expected, no measurable changes were observed in particle morphology after conjugation with folate, as evidenced by TEM (images not shown).

The folate-conjugated nanoparticles were incubated with KB cells, a human nasopharyngeal epidermal carcinoma cell line overexpressing the FR. As both samples contained the same molar concentrations of polymers and fluorescein probes, but different numbers of particles overall, quantification of cellular uptake on a polymer molar basis was observed. After 4 hours of incubation, confocal microscopy of the cells showed that the polymers were internalized to a higher extent when they were of a cylindrical morphology than when they were in the form of the spherical particles (Figure 3, a and d), despite the fact that the cylinders are much larger in volume compared the spheres (*ca*. 700 times difference in volume for an average cylinder *vs*. sphere, based on TEM volume calculations). This result is somewhat surprising because previously we have observed an opposite trend in cell internalization of the same nanostructures, with the exception that they were instead functionalized with the cell transduction domain peptide sequence of the HIV Tat protein (PTD).27 The different binding affinities between folate/FR and PTD/cell surface may contribute to the contrasting results for the folate- and PTD-decorated nanostructures. It is hypothesized that a larger structure may span across several FR binding sites and lead to an increase in polyvalent effect,28 and increased FR-mediated endocytosis. By contrast, the PTD-SCKs interact with the cell surface in a receptor-independent fashion29 and, therefore, may not benefit from polyvalency. For both nanostructure shapes, an excess of free folate (1 mmol/L) was able to competitively inhibit the binding and internalization of folate-functionalized particles, suggesting FR specific binding (Figure 3, b and e). The control experiments using particles that lacked surface folate showed significantly reduced cell uptake for both spherical and cylindrical particles (Figure 3, c and f).

These preliminary results suggest that cylinders are a better candidate for cell internalization when the mechanism involves a receptor-mediated endocytotic process. This conclusion is valid, at least, for the folate-FR pair, which achieved a high degree of cell uptake; however, it may not be general. Each individual target-receptor pair deserves its own study on the nanoparticle shape effect due to the difference in binding affinity, target density on cellular surfaces, *etc*. Knowing that shape plays important roles in cell internalization, as well as in overall biodistribution behavior *in vivo*,30 provides exciting opportunities to optimize another parameter in the design of drug delivery systems.

Acknowledgments

This material is based upon work supported by the National Heart Lung and Blood Institute of the National Institutes of Health as a Program of Excellence in Nanotechnology (HL080729) and by the National Science Foundation under grant no. 0451490. The authors thank Mr. G. M. Veith for TEM imaging.

References

1. Buruiana EC, Kowalczuk M, Adamus G, Jedlinski Z. J Polym Sci, Part A: Polym Chem. 2008; 46:4103–4111.
2. Chang C, Wei H, Quan CY, Li YY, Liu J, Wang ZC, Cheng SX, Zhang XZ, Zhuo RX. J Polym Sci, Part A: Polym Chem. 2008; 46:3048–3057.

NIH-PA Author Manuscript

NIH-PA Author Manuscript

NIH-PA Author Manuscript

3. Li G, Song S, Guo L, Ma S. J Polym Sci, Part A: Polym Chem. 2008; 46:5028–5035.
4. Liu Y, Huang K, Peng D, Liu S, Wu H. J Polym Sci, Part A: Polym Chem. 2007; 45:2152–2160.
5. Shabat D. J Polym Sci, Part A: Polym Chem. 2006; 44:1569–1578.
6. Rothenfluh DA, Bermudez H, O'Neil CP, Hubbell JA. Nature Nanotechnology. 2008; 7:248–254.
7. Champion JA, Mitragotri S. Proceedings of the National Academy of Sciences of the United States of America. 2006; 103:4930–4934. [PubMed: 16549762]
8. Chithrani BD, Chan WCW. Nano Letter. 2007; 7:1542–1550.
9. Rothberg KG, Ying YS, Kolhouse JF, Kamen BA, Anderson RG. Journal of Cell Biology. 1990; 110:637–649. [PubMed: 1968465]
10. Reddy JA, Leamon CP, Low PS. In Delivery of Protein and Peptide Drugs in Cancer. 2006:183–204.
11. Turek JJ, Leamon CP, Low PS. Journal of Cell Science. 1993; 106:423–430. [PubMed: 8270640]
12. Reddy JA, Abburi C, Hofland H, Howard SJ, Vlahov I, Wils P, Leamon CP. Gene Therapy. 2002; 9:1542–1550. [PubMed: 12407426]
13. Guy Z, Liliane ZI, Emmanuel D, Jean-Paul B. Angewandte Chemie (International ed in English). 2003; 42:2666–2669. [PubMed: 12813749]
14. Zuber G, Muller CD, Behr JP. Technology in Cancer Research & Treatment. 2005; 4:637–643. [PubMed: 16292883]
15. Kukowska-Latallo JF, Candido KA, Cao Z, Nigavekar SS, Majoros IJ, Thomas TP, Balogh LP, Khan MK, James R, Baker J. Cancer Research. 2005; 65:5317–5324. [PubMed: 15958579]
16. Rossin R, Pan D, Qi K, Turner JL, Sun X, Wooley KL, Welch MJ. Journal of Nuclear Medicine. 2005; 46:1210–1218. [PubMed: 16000291]
17. Bharali DJ, Lucey DW, Jayakumar H, Pudavar HE, Prasad PN. Journal of American Chemical Society. 2005; 127:11364–11371.
18. Dixit V, Van den Bossche J, Sherman DM, Thompson DH, Andres RP. Bioconjugate Chemistry. 2006; 17:603–609. [PubMed: 16704197]
19. Hu X, Chen X, Liu S, Shi Q, Jing X. J Polym Sci, Part A: Polym Chem. 2008; 46:1852–1861.
20. O'Reilly RK, Joralemon MJ, Hawker CJ, Wooley KL. J Polym Sci, Part A: Polym Chem. 2006; 44:5203–5217.
21. Ma Q, Wooley KL. Journal of Polymer Science Part A: Polymer Chemistry. 2000; 38:4805–4820.
22. Ma, Q.; Remsen, EE.; Christopher, G.; Clark, J.; Kowalewski, T.; Wooley, KL. Proceedings of the National Academy of Sciences of the United States of America; 2002. p. 5058-5063.
23. Guo W, Hinkle GH, Lee RJ. Journal of Nuclear Medicine. 1999; 40:1563–1569. [PubMed: 10492380]
24. Pan D, Turner JL, Wooley KL. Chemical Communications. 2003; 19:2400. [PubMed: 14587701]
25. Shukla S, Wu G, Chatterjee M, Yang W, Sekido M, Diop LA, Müller R, Sudimack JJ, Lee RJ, Barth RF, Tjarks W. Bioconjugate Chemistry. 2002; 14:158–167. [PubMed: 12526705]
26. Gabizon A, Horowitz AT, Goren D, Tzemach D, Mandelbaum-Shavit F, Qazen MM, Zalipsky S. Bioconjugate Chemistry. 1999; 10:289–298. [PubMed: 10077479]
27. Zhang K, Fang H, Chen Z, Taylor JSA, Wooley KL. Bioconjugate Chemistry. 2008 in press.
28. Hong S, Leroueil PR, Majoros IJ, Orr BG, James R, Baker J, Holl MMB. Chemistry & Biology. 2007; 14:107–115. [PubMed: 17254956]
29. Duchardt F, Fotin-Mleczek M, Schwarz H, Fischer R, Brock R. Traffic. 2007; 8:848–866. [PubMed: 17587406]
30. Geng Y, Dalhaimer P, Cai S, Tsai R, Tewari M, Miniko T, Discher DE. Nature Nanotechnology. 2007; 2:249–255.

NIH-PA Author Manuscript

NIH-PA Author Manuscript

NIH-PA Author Manuscript

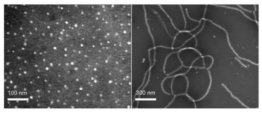

Figure 1.

TEM images (obtained on a carbon-coated copper grid with negative staining by a mixture of uranyl acetate) of (left) the spherical supramolecular assembly of PAA_{128}-*b*-PS_{40} formed in DMF by slow addition of water and (right) the cylindrical supramolecular assembly of PAA_{94}-*b*-PMA_{103}-*b*-PS_{28} formed in THF/water (vol:vol = 1:1) by slow addition of water. Both particles were shell-crosslinked with 2, 2′-(ethylenedioxy)bis(ethylamine), consuming nominally 20% of available carboxylic acids in the micelle.

NIH-PA Author Manuscript

NIH-PA Author Manuscript

NIH-PA Author Manuscript

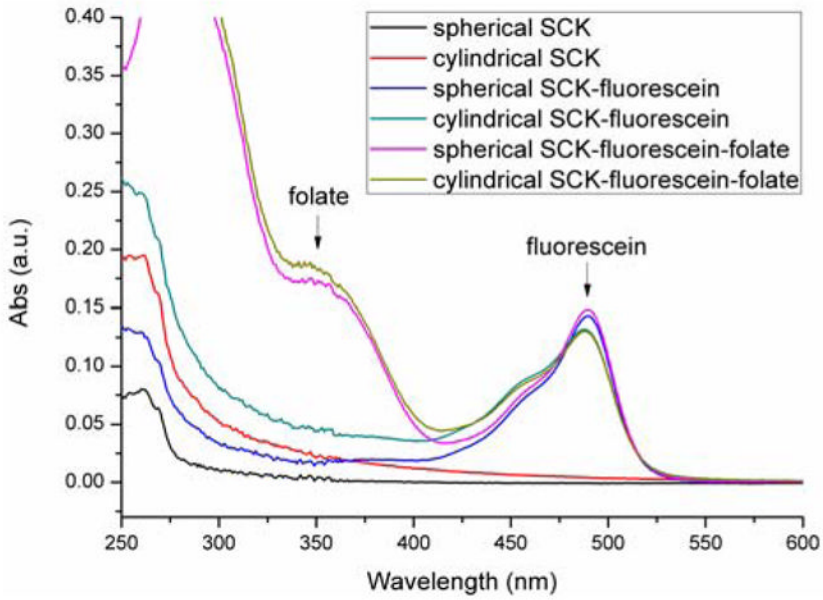

Figure 2.

UV-Vis spectra of the nanostructure carriers functionalized with fluorescent tag and folate. The absorbance at 488 nm represents fluorescein-5-thiosemicarbazide, the fluorescent tag. Approximately the same amount of fluorescein was coupled to each of the samples. The absorbance at 363 nm indicate successful coupling of folate-PEG-amine to the nanostructures. Using fluorescein-tagged SCKs as background, the absorbances at 363 nm for the folate-fluorescein-SCKs were used to calculate the number of folates per polymer chain.

NIH-PA Author Manuscript
NIH-PA Author Manuscript
NIH-PA Author Manuscript

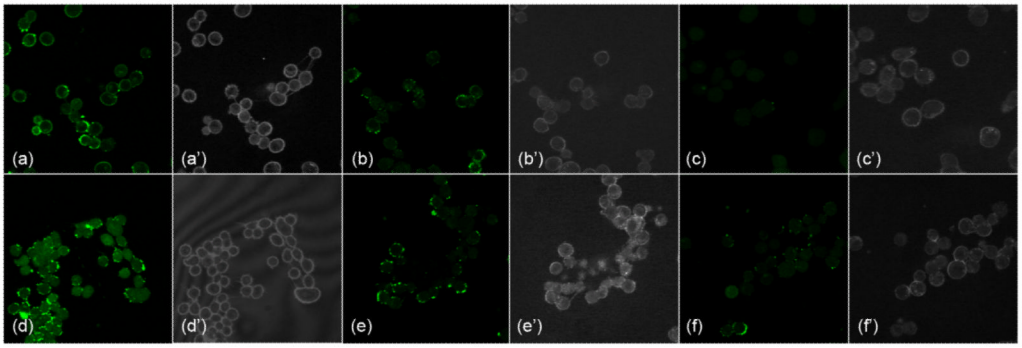

Figure 3.

Fluorescent confocal microscopy images of KB cells incubated for 4 hours at 37 °C with spherical and cylindrical nanoparticles functionalized with and without folate (70 nM polymer per 33-mm culture dish, plated with 3×10^5 cells per dish 24 h before imaging). All particles were tagged with equal amount of fluorescein-5-thiosemicarbazide. (a) folate-labeled spherical particle; (b) folate-labeled spherical particle with the addition of 1 mmol/L free folate; (c) spherical particles with no folate; (d) folate-labeled cylindrical particle; (e) folate-labeled cylindrical particle with the addition of 1 mmol/L free folate; (f) cylindrical particle with no folate; (a')-(f') bright field images corresponding to the fluorescent images.

NIH-PA Author Manuscript

NIH-PA Author Manuscript

NIH-PA Author Manuscript

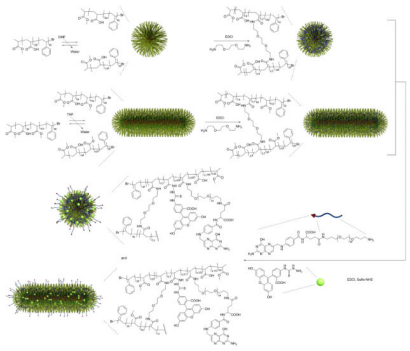

Scheme 1.

Synthesis of folate-functionalized shell-crosslinked nanoparticles of two distinct shapes. A post-nanoparticle functionalization strategy was used, in which the spherical and cylindrical nanoparticles were constructed first from discrete polymer chains, and then a folate-PEG derivative was conjugated to the surface of the nanoparticles. The nanostructures were also labeled by reaction with fluorescein-5-thiosemicarbazide to enable particle tracking.